

## 1. Research Objective

The goal of this project was to quantify organic aerosol precursor concentrations in an urban environment and to measure suitable organic photoproduct species that can act as tracers of photochemical processing to identify the occurrence and rate of secondary organic aerosol formation. Field measurements were made as part of the ASR field program Carbonaceous Aerosols and Radiative Effects Study (CARES) in June 2010. What is new in our approach is the measurement for the total concentration of long chain alkanes ( $>C_{10}$ ) and heavier alkyl substituted aromatics associated with diesel exhaust gas phase organic compound emissions. A method to measure these so called intermediate volatility organic compounds (IVOCs) was developed by modifying a proton transfer reaction mass spectrometer instrument to perform both volatile organic compound (VOC) and IVOC analysis by thermal desorption from a Tenax adsorbent trap (TD-PTR-MS). Lab and field results show that the TD-PTR-MS technique can measure long chain alkanes associated with diesel engine emissions and thus provide a novel means to measure these compounds to better understand the impact of vehicle emissions on secondary organic aerosol formation.

## 2. Research Progress and Implications

### TASK A. Analysis of IVOCs by PTR-MS.

1. Alkane Sensitivity Study: The PTR-MS response to n-alkanes was determined by preparing known mixtures with the dynamic dilution system in  $N_2$ . Alkanes undergo dissociative proton transfer reactions in the PTR-MS producing fragmentation patterns similar to electron impact ionization. **Figure 1** shows the fragmentation pattern for dodecane as an example of the typical pattern observed for n-alkanes. The  $C_8$ - $C_{16}$  n-alkanes produce a significant response and their spectra displayed similar features, yielding a similar relative abundance of fragment ions with the formula  $C_nH_{2n+1}$  for  $n \geq 3$ . For heptane and smaller n-alkanes there was little response and these species appear to be unreactive with  $H_3O^+$ . The n-alkane fragmentation pattern was a function of the PTR-MS drift tube field strength. At the lower field strengths there was less fragmentation into lighter ions. At 80 Td there was essentially no fragmentation to  $m/z$  41 and 43 while at 120 Td these were the most abundant ion fragments.

The benefit of operating at lower Td is that the n-alkane ion signal occurs at larger ion masses allowing for better distinction between IVOC and VOC species. Many VOC species are known to undergo dissociative proton transfer reactions in the PTR-MS and the ions  $m/z$  41, 43 and 57 are common fragment ions from a wide range of species and are typically the most abundant ion signals in PTR-MS analysis of urban air. **Table 1** shows the fraction of total ion signal that occurs for each fragment ion for  $C_8$ - $C_{16}$  n-alkanes at 80 Td. Most of the ion signal is at  $m/z$  57, 71, and 85. There would be significant interference from VOC compounds for ions at  $m/z$  57 (butenes) and  $m/z$  71 (penetenes, methacrolien, methyl vinyl ketone) and to use these ions to monitor for alkanes will require sampling discrimination to prevent VOC collection on the Tenax trap. The ions  $m/z$  85, 99, 113, and 127 may be more unique tracers of long chain alkane abundance in the atmosphere.

The PTR-MS instrument's sensitivity to alkanes was determined by preparing known n-alkane and toluene mixtures using the dynamic dilution system. The alkane species of interest was co-injected with toluene to ensure the syringe pump was operating correctly, since an expected signal for toluene can be calculated. The n-alkane sensitivity is shown in **Figure 2**. The response curve displays a dependence on the drift field strength. Our data reveal that the PTR-MS is insensitive to alkanes with carbon numbers  $< C_7$ . The increase in sensitivity

for alkanes  $> C_7$  is consistent with the rate constant measurements of Arnold et al., (1998) which are also shown in the figure. Quantum mechanical calculations of alkane C-C bond proton affinities (PA) reveal that the more central bonds of the molecule have the largest proton affinities and for larger alkanes approach that of water at 165.5 kcal/mole (Hunter and East, 2002). The  $H_3O^+$  + n-alkane reactions appear to be endothermic and explains why the n-alkane sensitivity is significantly lower than that of toluene. The normalized sensitivity for dodecane at 80 Td was 2.8 Hz per ppbv per MHz  $H_3O^+$  (ncps) compared to 13 ncps for toluene. The PA of n-alkanes appears to plateau for larger alkanes and the 120 Td sensitivity curve suggests a sensitivity plateau as well for n-alkanes  $> C_{14}$ . At the 80 Td condition the n-alkane sensitivity is lower than expected. Given the factor of 1.6 increase in reaction time one would expect the sensitivity at 80 Td to be a factor of 1.6 greater than at 120 Td as was observed for toluene. The lower n-alkane sensitivity for the lower drift field strength is consistent with an endothermic reaction. The lower  $H_3O^+$  ion energies at 80 Td result in a lower reaction rate. The n-alkane response curve at 80 Td displayed a different shape than the 120 Td condition. This difference was attributed to the greater number of higher m/z ions at the 80 Td condition and their lower transmission efficiency through the mass spectrometer. At 120 Td the n-alkane sensitivity is primarily determined by the ion signal at m/z 41, 53 and 57 ions. At 80 Td the sensitivity is determined by broader range on ion masses as shown in **Table 1**. The ion signal for alkanes  $< C_7$  is likely due to alkane reactions with  $O_2^+$  and  $NO^+$  in the drift tube since these alkanes have low proton affinities and should not react with  $H_3O^+$ . Preliminary tests have shown that iso-alkanes (ie. 2-methylundecane) display similar fragmentation patterns and sensitivity as n-alkanes.

2. Design and Construction of IVOC Sampling System: **Figure 3** shows a diagram of the thermal desorption sampler used to collect IVOC compounds. The PTR-MS (Ionicon Analytik) drift tube was modified to have 2 inlets, one for the IVOC thermal desorption sampler and one for VOCs. The thermal desorption sampler used Tenax TA adsorbent resin, providing a means to preconcentrate organic compounds to improve detection, and to provide a means to discriminate against the collection of volatile organic compounds that can interfere in the interpretation of the PTR-MS mass spectrum. Approximately 0.175 grams of Tenax TA was packed into a 0.172 cm (0.0675") ID stainless steel tube. The tube was resistively heated with an AC current and temperature controlled using a phase angle control module (Nu Wave Technologies) controlled by a PID algorithm. Mass flow controllers were used to regulate the sample, desorption, and back flush flows through the adsorbent. Dry nitrogen gas was used for desorption and back flush. The Tenax trap was connected to a heated 2-position six port gas sampling valve (VICI Valco). Another heated multistage 4-port valve was used as a stream selector to sample ambient air or zero air (dry  $N_2$ ). The sampler was controlled by a software program (Azeotech DaqFactory) that allowed for automation of the sampling and thermal desorption steps. The Tenax trap was connected to a custom made sample ring on the PTR-MS drift tube by a 0.0254 cm (0.01") ID tube. The trap was positioned directly above the PTR-MS drift tube and electrically isolated from the sample drift ring. The drift tube was thermostated to 70 °C using the thermoelectric drift tube heater supplied by Ionicon. For analysis of heavier organics a high temperature resistive glass drift tube would be preferred such as used in Thornberry et al. (2009). Because of limitations on drift tube temperature that could be obtained with our system, the sampling lines, either electropolished stainless steel tubing (UHP Cardinal) or silica coated stainless steel tubing (Sulfinert, Restek Corp), were heat traced to a similar temperature (80 °C), so that the drift tube didn't act as a cold spot and become contaminated. The setup allowed for easy switching between the VOC sampling and IVOC desorption sampling with minimal disruption of the drift tube pressure. While the IVOC sample is being collected, the IVOC inlet is shut (S1 closed) and the VOC inlet is open (S2 open) to allow for VOC measurement.

Instrument control software and electronics for control of the thermal desorption system were designed and built. Initial desorption tests established that the detection limit for p-xylene and dodecane, for example, would be  $\sim 0.07 \text{ ug/m}^3$  ( $\sim 0.015 \text{ ppbv}$ ) and  $\sim 4.2 \text{ ug/m}^3$  ( $\sim 0.55 \text{ ppbv}$ ) respectively for a 1.2-L air sample. This is more than sufficient sensitivity for measuring IVOC compounds in urban air. The reason for the higher detection limit of dodecane can be accounted for by two variables. The first is that the sensitivity of dodecane is  $\sim 4$  times lower than that of p-xylene. The second is the fragmentation of dodecane divides the signal into between multiple ions. Looking at **Table 1** it can be observed that 22% of the signal is found at  $m/z$  85. If we base our dodecane concentration on the  $m/z$  85 signal the fragmentation increases the detection limit by a factor of 5. In combination, these two variables increase the dodecane detection limit by a factor of 20. If these problems did not exist, the factor of 20 can be applied to the above detection limit to estimate an ideal case detection limit for dodecane. The  $4.2 \text{ ug/m}^3$  detection limit is equivalent to  $0.21 \text{ ug/m}^3$ , which is comparable to that observed for p-xylene.

3. Mass Spectra of Fuel and Exhaust: In order to determine how the PTR-MS responds to vehicle fuel and exhaust a number of experiments were performed. Initially the fuels were measured by injecting a small liquid volume at a low infusion rate into a hot manifold and diluted by a large flow of dry nitrogen. This mixture was measured by the VOC inlet of the PTR-MS and the resulting spectra can be observed in **Figure 4**. Both fuels are dominated by alkanes and aromatics. A major difference between the fuels is apparent in the larger species. The diesel fuel spectra extends out to  $m/z$  240 while the gasoline stops before  $m/z$  180. There are a lot more heavy organics found within the diesel fuel. Another major feature is evident in the abundance of the family denoted by the red bars. While present in both fuels, it is much more abundant in the diesel fuel and could act as a great indicator of diesel exhaust.

The next step was to observe the exhaust from gasoline and diesel engines. A series of chambers tests were performed at the Lovelace Respirator Research Institute in Albuquerque, NM by flowing engine exhaust into chambers at controlled concentrations. The exhaust was then measured by both the VOC and IVOC inlet. If operated in the right conditions, the PTR-MS can be used as a tool to measure gasoline and diesel emissions separately. On the VOC side, the air was sampled through a cold trap. The purpose of the cold trap is to remove water vapor from the sample to improve the sensitivity of the instrument. The air sample goes through a tube kept at  $-30 \text{ C}$ . This cold zone also acts as a trap for heavy organics, with species with low vapor pressures sticking to the walls more readily. **Figure 5** is the resulting spectra of both vehicle exhausts. The main point to observe is the similarity between the two exhausts. This is a surprising result as the fuels have many different features, but the exhausts generally have similar abundances of all the species. This similarity can be attributed to the removal of the heavy organics from the diesel exhaust. The diesel spectra extends farther into heavier organics than the gasoline exhaust, but it is not nearly as prominent as it is within the fuels.

The real differences between the exhaust can be observed through the IVOC system when the sample is treated with a high temperature purge. In order to observe the discrimination achieved through purge mode, all the  $m/z$  signals were normalized to  $m/z$  135. The  $m/z$  135 signal was chosen as the normalizing agent because it is a relatively abundant signal in both exhausts and limited discrimination/loss is expected at this  $m/z$  value. Transforming the data in this manner allows the evaluation of relative changes between  $m/z$  signals. The

valuable data with this mode comes from the ratios observed between different ions. As different levels of discrimination are implemented (higher purge temperatures) the ratio between two ions is expected to change. The change in this ratio signifies more discrimination against one ion than the other. For example, the ratio of  $m/z$  121 to  $m/z$  85 of diesel exhaust in the IVOC mode under a 30 °C purge is 0.28. When the purge temperature is increased to 150 C the ratio changes to 1.59. These ratios can be used to distinguish gasoline exhaust from diesel exhaust. Under the 150 C purge temperature the ratio observed in the gasoline was 60, which is almost a factor of 40 higher than the ratio of 1.59 observed in the diesel exhaust. This result is consistent with the differences in fuel composition. Within the gasoline exhaust the  $m/z$  85 signal is dominated by C8 and lighter organics and the  $m/z$  121 signal is dominated by C3-benzenes. Gasoline contains very few alkanes that are observable by a PTR-MS, so it is inherent that the  $m/z$  121 to  $m/z$  85 ratio will be much greater than 1. Conversely, in the diesel exhaust the  $m/z$  85 signal is dominated by C9 and heavier organics while the  $m/z$  signal is still dominated by C3-benzenes. Diesel fuels is mostly composed of alkanes observable by the PTR-MS and large aromatics, which means the  $m/z$  121 to  $m/z$  85 ratio will be much closer to 1 than the gasoline. This will result in different ratios for each exhaust, which may help quantify the relative contribution of diesel and gasoline to complex vehicle exhaust mixtures.

4. IVOC Sensitivity – Comparison with VOC Sampling Mode: In order to test the reliability of the IVOC system, the desorption peak area was compared to the corresponding area observed in the VOC side. **Figure 6** is the comparison of trimethylbenzene observed during both modes. The data product from the IVOC measurement is achieved through taking the area of the desorption peak to get an area counts measurement. In order to compare this to the VOC mode we need to calculate the area counts observed by the VOC mode. This is done by averaging the signal observed during the IVOC sample collection and multiplying it by the sample time to get a VOC area counts. The area counts observed in Figure 6 are 50,045 for the VOC and 88,423 for the IVOC. These values are different due to the difference of sample flow rates. The VOC mode samples at 25 sccm and the IVOC mode at 42 sccm. In order to account for this, the VOC area counts need to be multiplied by the ratio of these two flow rates. Multiplying 50,045 by 42/25 translates the VOC area counts to 84,074. Now comparing the IVOC to VOC area counts a difference of ~5% is observed, which leads to good agreement between the two sampling methods. These areas compare to within 5% of one another, which shows that the IVOC system generates comparable concentrations to those measured by the VOC mode.

5. IVOC Discrimination of Interfering VOCs: By implementing a purge mode we can discriminate against light VOCs. **Figure 7** shows the desorption peaks of VOCs with varying Tenax breakthrough volumes. The four species were put under two purge temperatures, 30 °C and 150 °C. Under the 30 °C scenario the volume of gas passes through the Tenax does not exceed the breakthrough volume of any of the four species, so no discrimination would be expected. This is represented by the blue trace in **Figure 8**. Conversely, under the 150 °C purge temperature the breakthrough volumes of all compounds is significantly reduced, which will result in large discrimination against the VOCs. This is represented by the red trace. Large discrimination against the lighter VOCs can be observed with the methacrolein and toluene signals decreasing by 99% and 89% respectively. The p-xylene and trimethylbenzene were discriminated less than the lighter VOCs, but still show significant reduction in the signals. Toluene and octane have similar desorption volumes, if we can purge toluene octane should be purged as well. Approximately 90% of alkanes in gasoline are octane and lighter.

Therefore, the purge mode should help discriminate against gasoline alkanes, eliminating or vastly reducing their interference.

### **TASK B. Analysis of VOCs and Oxidation Products by GC-MS**

1. The cryogenic preconcentration system was integrated with the gas chromatograph ion trap system and tests were performed to determine if photochemical reaction products could be measured. It was determined that CO<sub>2</sub>, trapped by the liquid N<sub>2</sub> cryogen, was problematic for the ion trap, causing very poor sensitivity and poor chromatographic performance for the early portion of the chromatogram. Tests were conducted to try to remove CO<sub>2</sub> by chemical trapping and by sublimation from the cryo trap but we concluded the best approach was to abandon cryo trapping with the ion trap and instead use a thermal desorption based preconcentration system. This approach prevents CO<sub>2</sub> from being collected. We have built a new 2-channel preconcentration system based on thermal desorption. One channel will measure C<sub>2</sub>-C<sub>6</sub> hydrocarbons by trapping on a carbon sieve based resins cooled to -20 °C. The other channel will measure C<sub>5</sub>-C<sub>12</sub> volatile organic compounds by trapping onto a Tenax adsorbent. C<sub>2</sub>-C<sub>6</sub> hydrocarbons will be detected by flame ionization, while C<sub>5</sub>-C<sub>12</sub> VOC will be detected by the ion trap mass spectrometer.
2. We identified a list of photochemical products to identify for the CARES field campaign. These compounds are 2- and 3-pentanone (from n-pentane), 2,3-butadione (from o-xylene), o-cresol (from toluene), and 2,5-dimethylphenol (from p-xylene). However these species could not be identified in the CARES chromatograms likely due to these compounds being below instrument detection limits as the meteorology of the CARES field experiment was such that high concentration photochemical pollution events were not observed.

### **TASK C. CARES Field Experiment**

The PTR-MS and GC-ITMS were deployed at the T0 site at American River College. WSU LAR's role was expanded through inclusion of our Mobile Atmospheric Chemistry Laboratory (a 20 foot shelter) and additional measurements of gas phase species (NO, NO<sub>2</sub>, NOy, CO, O<sub>3</sub>), PM size distribution, and meteorological measurements for the T0 site through subcontract with ACREF. VOC data from the GC-MS and PTR-MS along with other gas phase data and meteorological measurements were archived with the ARM as part of the CARES data archive.

IVOC data was successfully collected for a 2 week period in CARES. A series of ions were selected for monitoring in the CARES field campaign. The ions m/z 93, 121 and 135 were selected to measure alkylbenzene abundance with the intention of comparing the IVOC response for these ions to the VOC mode response. To test the accuracy of the IVOC desorption system in the field, a peak area calibration curve was developed for toluene (m/z 93) using the same gas standard utilized during the calibrations of the standard VOC inlet. The calibration was then applied to the m/z 93 peak areas measured in IVOC mode and compared to the toluene concentrations measured in VOC mode. A plot of VOC measured toluene vs. IVOC measured toluene yielded a slope of 0.44 and an r<sup>2</sup> of 0.79 resulted when the fit was forced through zero. This was also performed for the m/z 121 and 135 ions yielding slopes of 0.56 and 0.59 respectively and r<sup>2</sup> values of 0.73 and 0.6 respectively. This does not show reasonable agreement between the two systems with the IVOC method underestimating concentrations. However, this underestimation is expected due to the purge/discrimination mode implemented during the IVOC mode. The level of discrimination has not yet been well quantified for the CARES operations, but early estimates

have shown that the discrimination could be on the order of up to 50% for these compounds. Looking at the slopes, if 50% of the compound was purged from the Tenax before IVOC sampling then this would explain the underestimation of the IVOC mode. Further investigation is required in order to ascertain the accuracy of IVOC field measurements, but the initial results are promising.

The ions 57, 71, 85, and 99 ( $C_nH_{2n+1}$ ) were chosen to measure alkane abundance. The area count response for these ions together with  $NO_x$  mixing ratios averaged over the IVOC sampling time are shown in **Figure 9**. In general the ions covaried with each other and tracked variations in  $NO_x$ . The  $m/z$  57 and 71 ions displayed greater diel variability than the  $m/z$  85 ion, especially in the later part of the measurement period and likely indicates that species other than long chain alkanes produce significant ion signal at these masses. The  $m/z$  99 ion displayed the overall highest count rates, with the largest count rates occurring during a pollution episode on June 28. The IVOC alkane concentrations were calculated from the sum of  $m/z$  57, 71, 85 and 99 ion signals intensity using a whole diesel fuel response factor for  $C_{12}$ - $C_{18}$  alkanes determined *post facto* in laboratory experiments. The resulting alkane concentration time series is displayed in **Figure 10** along with total alkylbenzene species concentration measured by the PTR-MS in VOC mode. These species include toluene,  $C_2$ -alkylbenzenes (xylenes and ethylbenzene) and  $C_3$ -alkylbenzenes (trimethylbenzene isomers, ethyltoluene isomers, propylbenzene isomers), and are good tracers of spark ignition vehicle exhaust and important SOA precursors. The total alkane mixing ratio determined by TD-PTR-MS was about  $\frac{1}{2}$  the total VOC alkylbenzene mixing ratio. The data suggest that IVOC alkanes are in significant abundance and would be important SOA precursors.

The ions 97, 111, 125, and 139 from the  $C_nH_{2n-1}$  group were also monitored and their response is displayed in **Figure 11** along with measured mixing ratios of  $C_2$ - and  $C_3$ -alkylbenzenes measured in VOC mode. We note that nopinone, a product of the ozone reaction with  $\beta$ -pinene, also occurs at  $m/z$  139 and may be an interference. There was significant signal for the  $m/z$  97, 111, and 125 ions. These ions were observed in both diesel fuel and gasoline and may be relative unique tracers of engine exhaust as there are few VOC species that produce ions at these masses in the PTR-MS. In general there was a good correlation between these masses and they displayed a similar pattern of variability as the  $C_nH_{2n+1}$  ion group. The  $m/z$  97 ion displayed the largest response of this group. During the clean air period experienced on June 20 the response of the  $C_nH_{2n-1}$  and the  $C_nH_{2n+1}$  ions were often at the detection limit of the method. Elevated counts for all these ions were observed on June 17, 21, and 28 corresponding to periods of elevated  $NO_x$  and  $C_2$  and  $C_3$ -alkylbenzenes. The similarity in temporal variability of these ion groups and their correspondence with  $NO_x$  and alkylbenzene variation suggests these ion groups represent species emitted in roadway exhaust. **Figure 12** shows the correlation between the  $m/z$  85 and 97 ions. The slope of the plot was 0.74 with an  $r^2$  of 0.880. The observed ambient ratio between these ions lies in between the ratios observed in vehicle exhaust at low (30 C) and high (150 C) purge conditions. The discrimination conditions implemented during CARES were different from the ones performed on vehicle exhaust. The level of discrimination achieved during CARES has not yet been well quantified, but the purge was performed at 100 °C and is expected to lie between the low and high purge conditions tested with the vehicle exhausts. At higher purge temperatures, the  $m/z$  ratios in diesel and vehicle exhaust become quite different. Observing these  $m/z$  ratios may prove to be a way to determine impact of diesel engine emissions on hydrocarbon abundance, but further investigation is required.

#### 4. Information Access

The following lists presentations / publications of work from this project:

Quantification of diesel fuel semi-volatile organic compounds by proton transfer reaction mass spectrometry, M.H. Erickson, B.T. Jobson, and D.H. Garvey, 2010 Atmospheric Systems Research annual meeting in Bethesda, MA.

*Quantification of Diesel Fuel Intermediate-Volatile Organic Compounds by Proton Transfer Reaction Mass Spectrometer*, M.H. Erickson, B.T. Jobson, American Geophysical Union Fall Meeting, San Francisco, Dec 13-17, 2010.

*SOA precursors at the T0 site during the 2010 CARES campaign*, A21C-0074-P, H.W. Wallace, B.T. Jobson, M.H. Erickson, American Geophysical Union Fall Meeting, San Francisco, Dec 13-17, 2010.

A manuscript, *Quantification of diesel exhaust gas phase organics by a thermal desorption proton transfer reaction mass spectrometer*, M. H. Erickson, H. W. Wallace, and B. T. Jobson, was submitted for publication to Atmospheric Chemistry and Physics journal in 2012. The submission was withdrawn after reviewers suggested separating the technical approach from the CARES field results. This was done and a manuscript on the technical approach was submitted to Atmospheric Measurement Techniques in 2013 and is currently in the final review process: *Measuring long chain alkanes in diesel engine exhaust by thermal desorption PTR-MS* M. H. Erickson, M. Gueneron, and B. T. Jobson, Atmos. Meas. Tech. Discuss., 6, 6005–6046, 2013.

**Tables**Table 1. The percentage of total ion abundance of fragment ions  $C_nH_{2n+1}$  from n-alkanes at 80 Td.

<b>n</b>	<b>m/z</b>	<b>C8</b>	<b>C9</b>	<b>C10</b>	<b>C11</b>	<b>C12</b>	<b>C13</b>	<b>C14</b>	<b>C15</b>	<b>C16</b>
<b>3</b>	<b>43</b>	4%	3%	2%	2%	1%	1%	1%	1%	2%
<b>4</b>	<b>57</b>	39%	21%	24%	28%	27%	26%	25%	24%	24%
<b>5</b>	<b>71</b>	41%	44%	30%	25%	24%	23%	22%	22%	21%
<b>6</b>	<b>85</b>	13%	26%	33%	26%	22%	20%	18%	17%	18%
<b>7</b>	<b>99</b>	1%	3%	7%	11%	10%	9%	8%	8%	7%
<b>8</b>	<b>113</b>	1%	0%	2%	5%	8%	8%	8%	7%	6%
<b>9</b>	<b>127</b>		2%	0%	2%	4%	7%	7%	7%	6%
<b>10</b>	<b>141</b>			1%	0%	1%	3%	6%	6%	5%
<b>11</b>	<b>155</b>				1%	0%	1%	2%	4%	4%
<b>12</b>	<b>169</b>					1%	0%	1%	2%	3%
<b>13</b>	<b>183</b>						1%	0%	0%	1%
<b>14</b>	<b>197</b>							1%	0%	1%
<b>15</b>	<b>211</b>								1%	0%
<b>16</b>	<b>225</b>									1%



## Figures

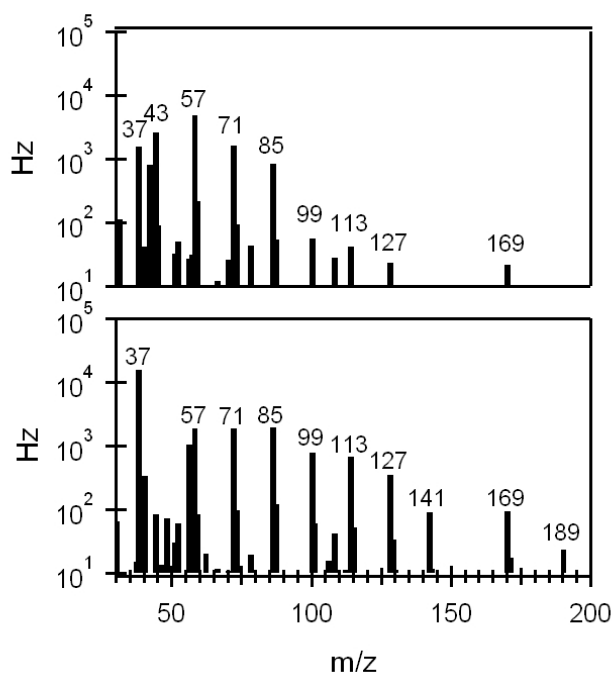


**Figure 1.** PTR-MS mass spectrum of dodecane at 120 Td (upper panel) and 80 Td (lower panel) drift tube conditions.

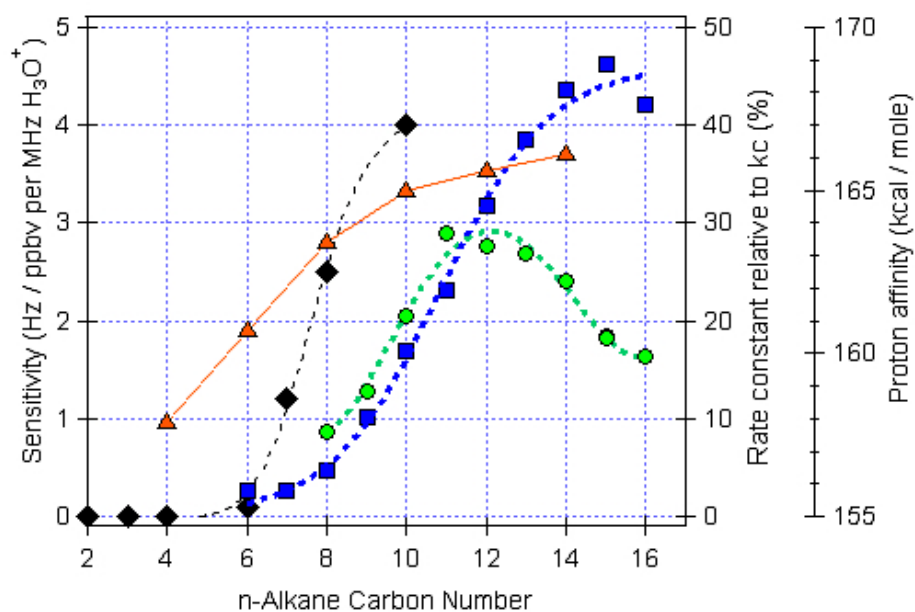


**Figure 2.** Alkane sensitivity (left axis) for 120 TD (blue squares) and 80 Td (green circles) compared to measured  $\text{H}_3\text{O}^+$  + alkane rate coefficients (black diamonds) by Arnold et al. (1998) expressed as a percentage of collision rate limit (right axis). Also shown is the proton affinity (red triangles) determined by Hunter and Elias (2002).

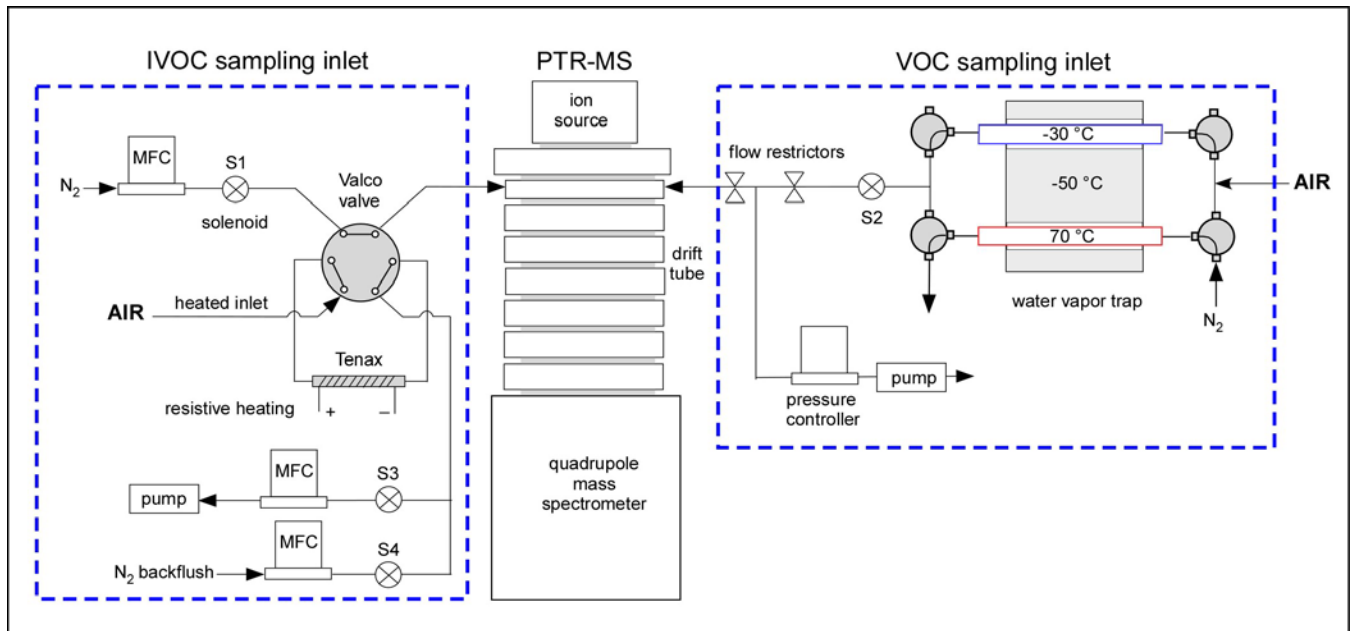


**Figure 3.** Plumbing schematic showing thermal desorption sampler for IVOC compounds and VOC sampling system with water vapor trap.

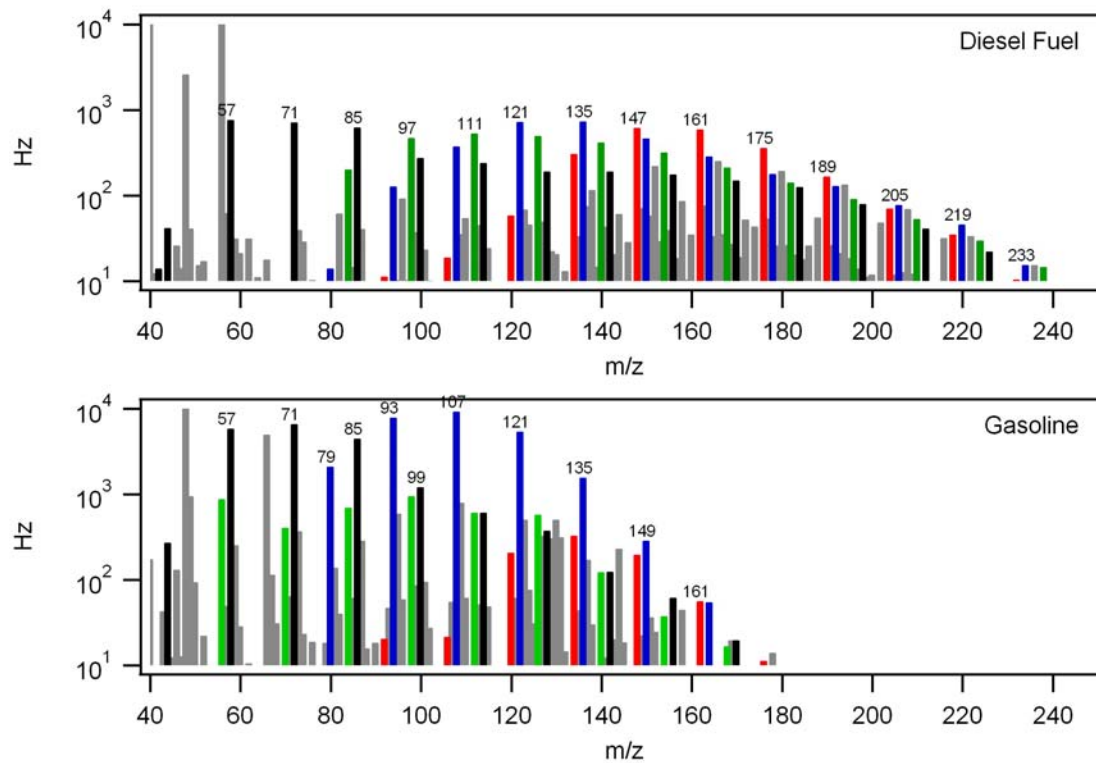


**Figure 4.** Mass spectrum of #2 diesel fuel and gasoline at 80 Td. Ion signal has been color coded to assign ions to common fragmentation patterns that identify common organic compound classes (black=alkanes, blue=aromatics, green=C<sub>n</sub>H<sub>2n-1</sub>, red=tetrahydro-naphthalenes). For diesel the ion signal is more evenly distributed across the 4 ion fragmentation groups than gasoline, while for the gasoline most of the ion signal was observed in the alkylbenzene group since the PTR-MS is insensitive to most of the light alkanes found in gasoline.

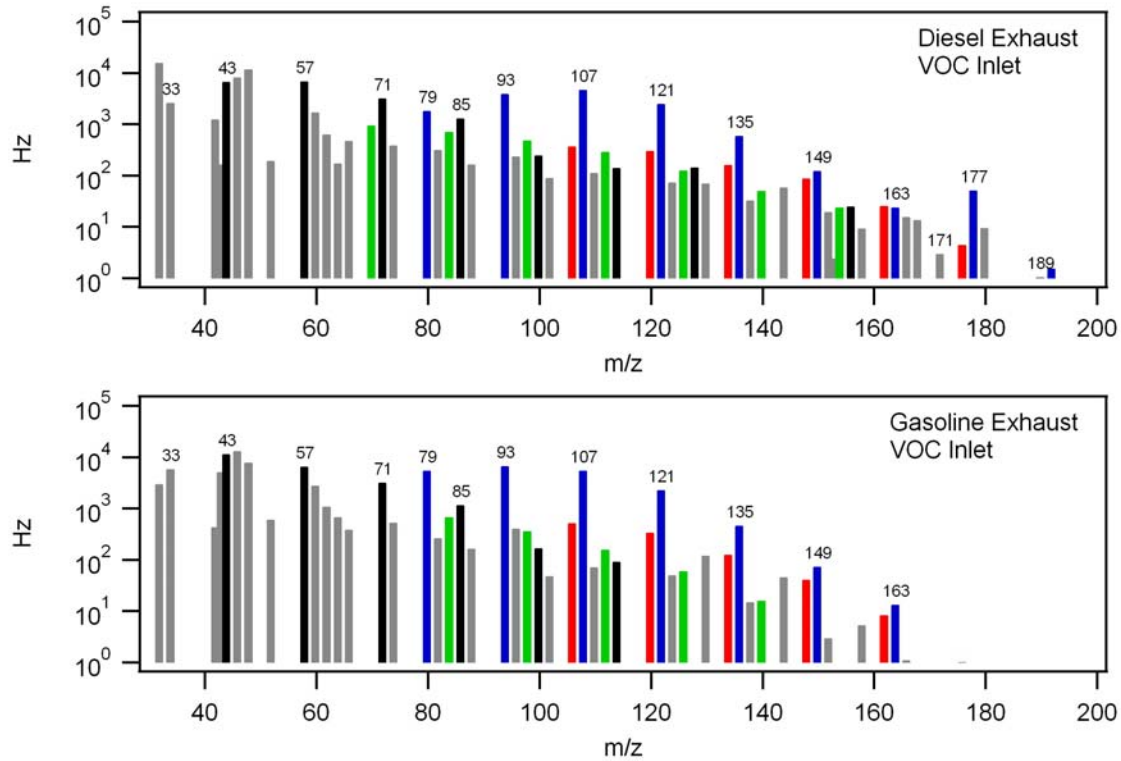


**Figure 5.** Vehicle exhaust measured through the cold trap (-30 C zone) with the VOC inlet. Ion signal has been color coded to assign ions to common fragmentation patterns that identify common organic compound classes (black=alkanes, blue=aromatics, green=C<sub>n</sub>H<sub>2n-1</sub>, red=tetrahydro-naphthalenes).

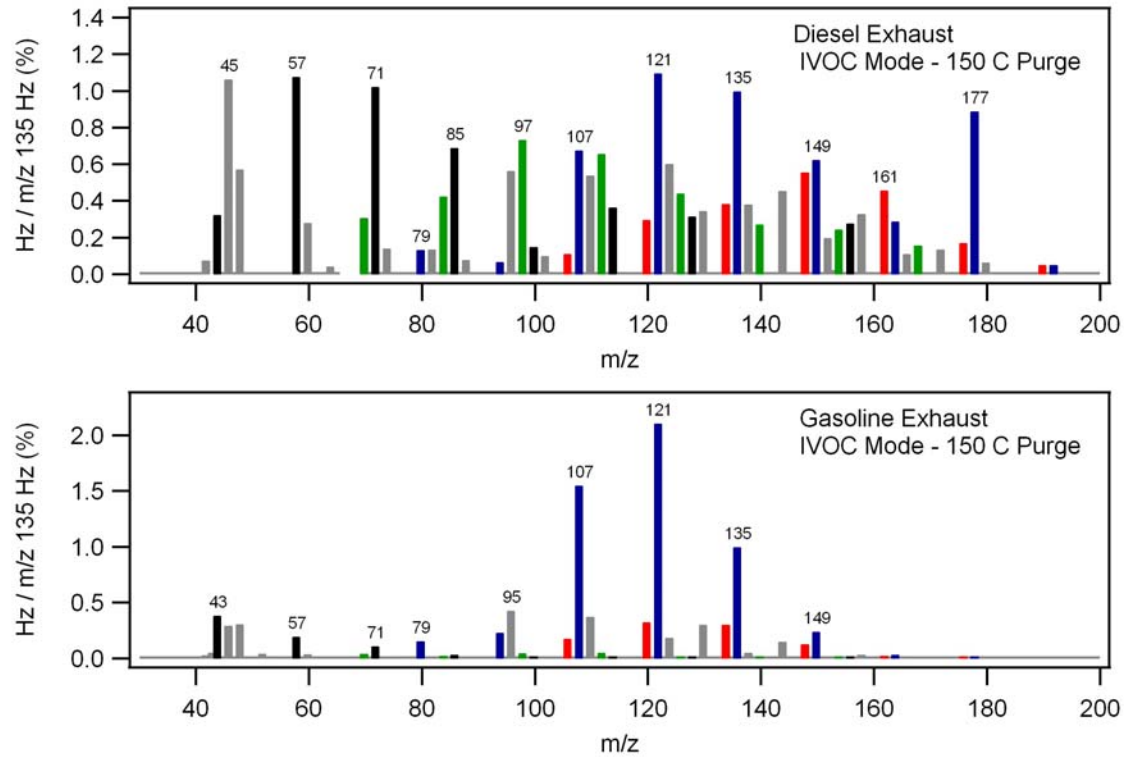


**Figure 6.** Vehicle exhaust measured with the IVOC thermal desorption system normalized to m/z 135 signal. Ion signal has been color coded to assign ions to common fragmentation patterns that identify common organic compound classes (black=alkanes, blue=aromatics, green=C<sub>n</sub>H<sub>2n-1</sub>, red=tetrahydro-naphthalenes).

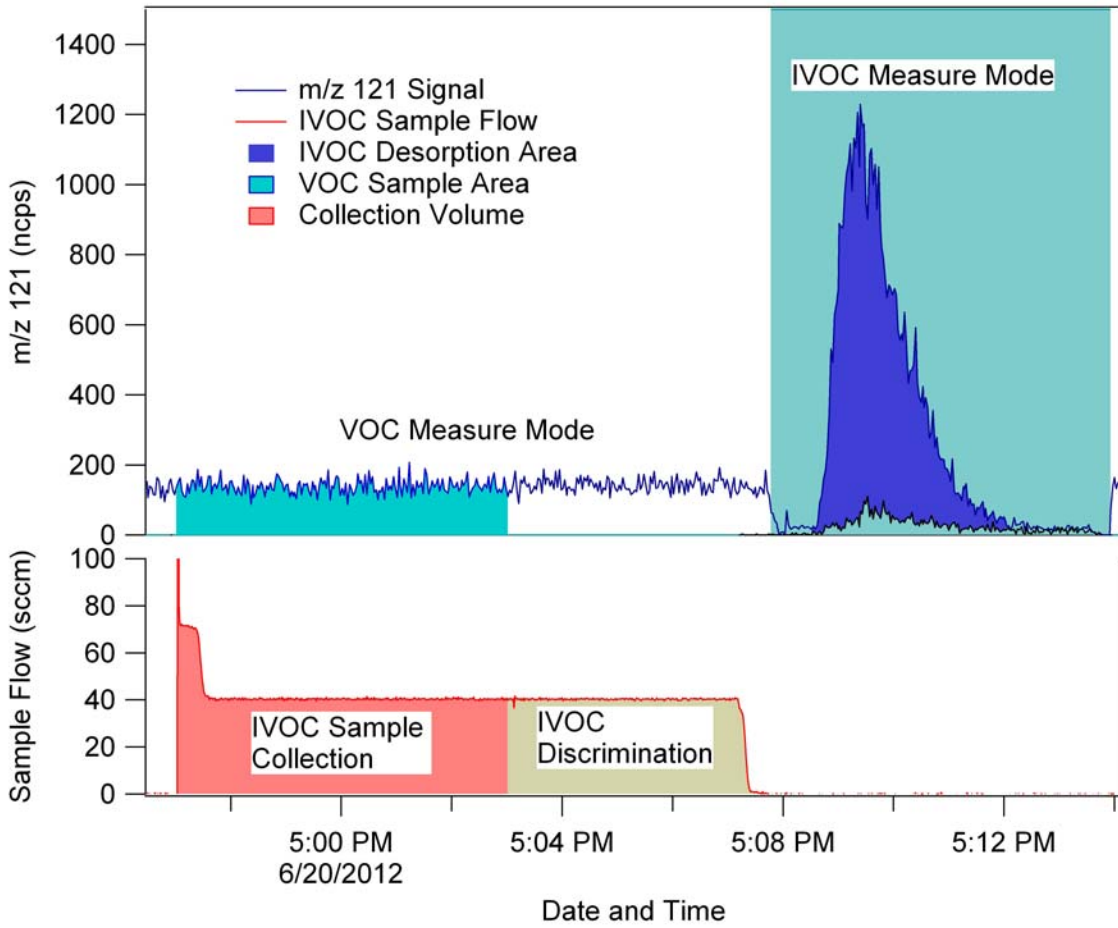
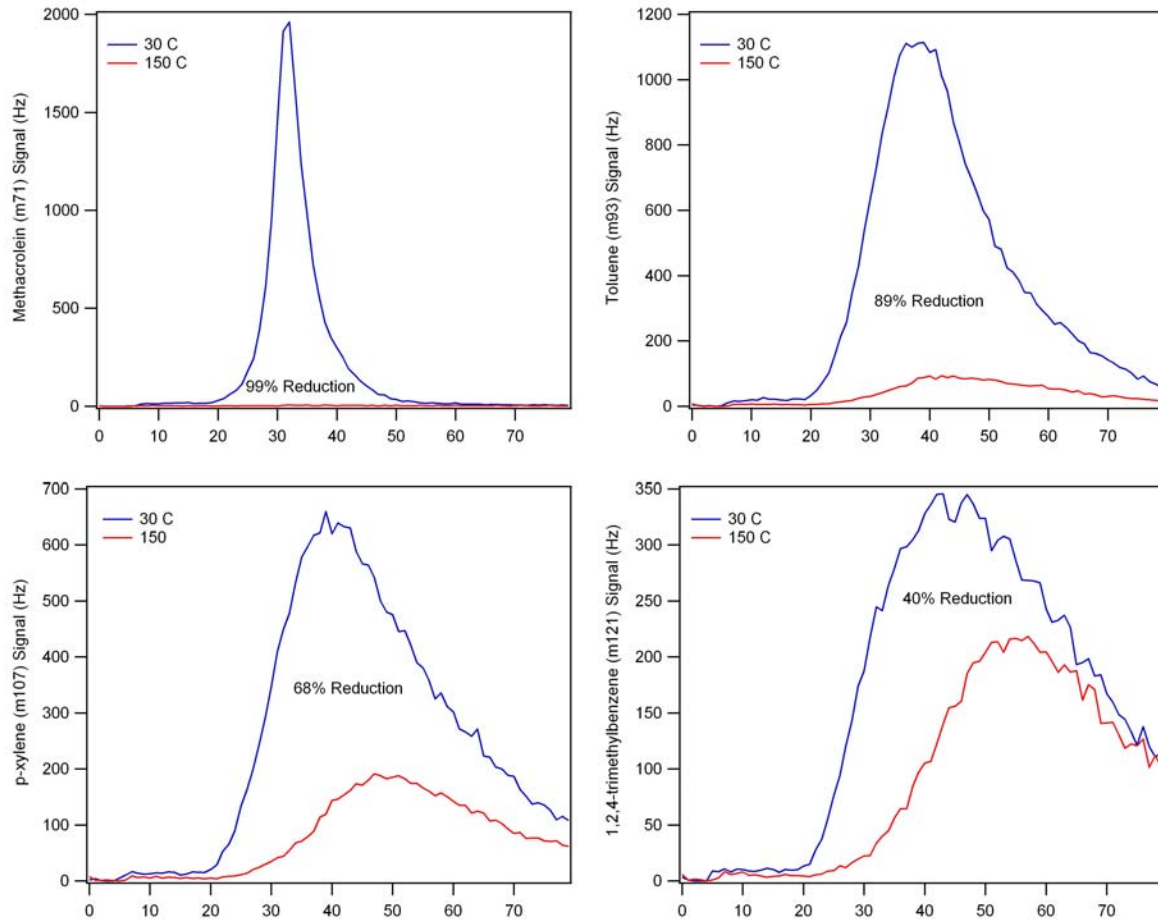
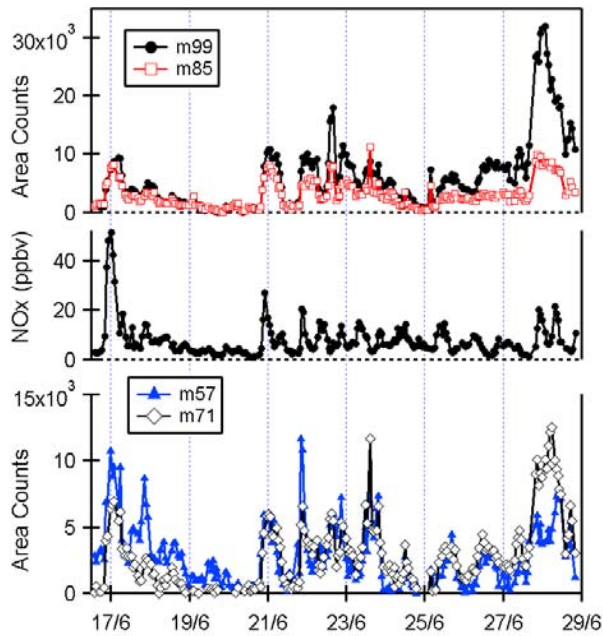


Figure 7. VOC/IVOC Comparison



**Figure 8.** VOC discrimination experiments showing impact of 150 °C purge that removes volatiles from the Tenax trap.



**Figure 9.** Time series of  $C_nH_{2n+1}$  group ion response measured in IVOC mode during CARES.  $NO_x$  mixing ratios averaged over the 30 minute IVOC sampling period are also shown.

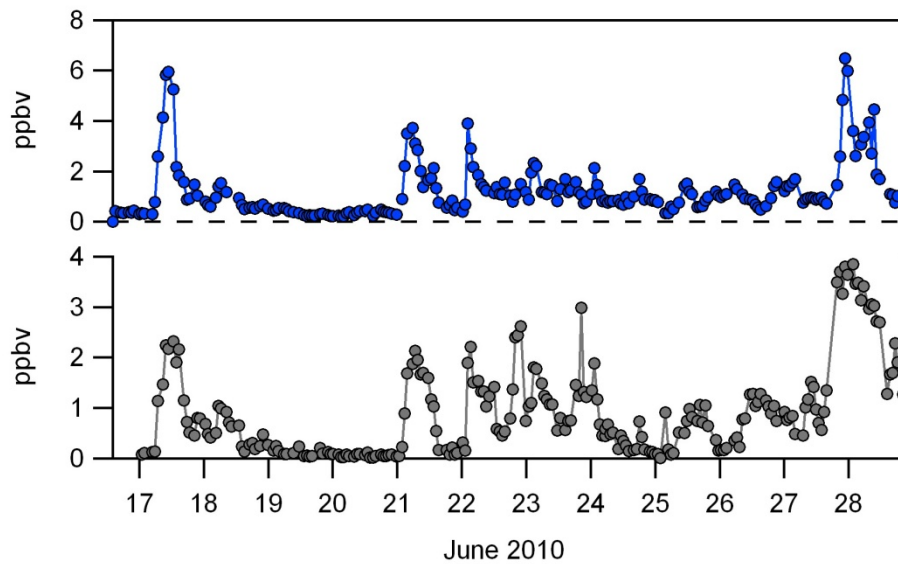


**Figure 10.** Total IVOC alkane concentration (bottom panel) determined from the sum of  $m/z$  57, 71, 85 and 99 ion signals measured with the IVOC sampler compared to the total alkylbenzene concentration (top panel) from the sum of  $m/z$  79, 93, 107, and 121 ion signals (top panel) measured with the dehumidifier.



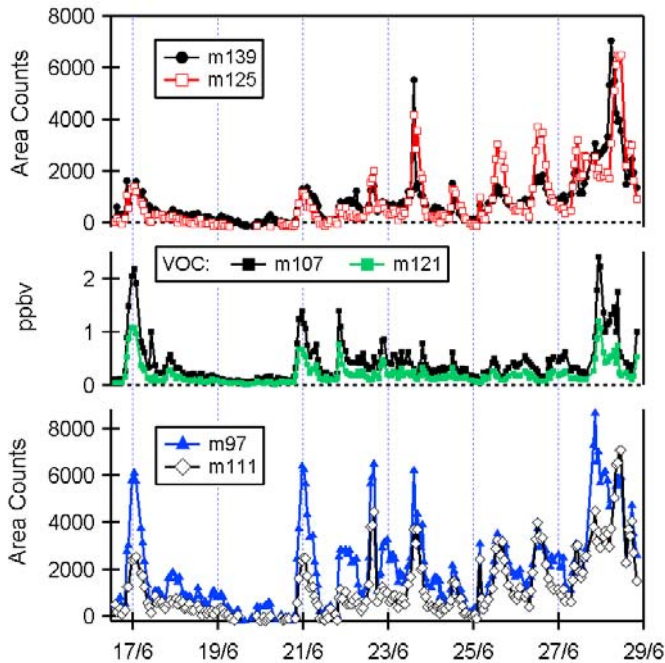


**Figure 11.** Time series of  $C_nH_{2n-1}$  group ion response measured in IVOC mode during CARES. Shown in the middle panel are mixing ratios of  $C_2$ -alkylbenzenes (m/z 107) and  $C_3$ -alkylbenzenes (m/z 121) measured in VOC mode.

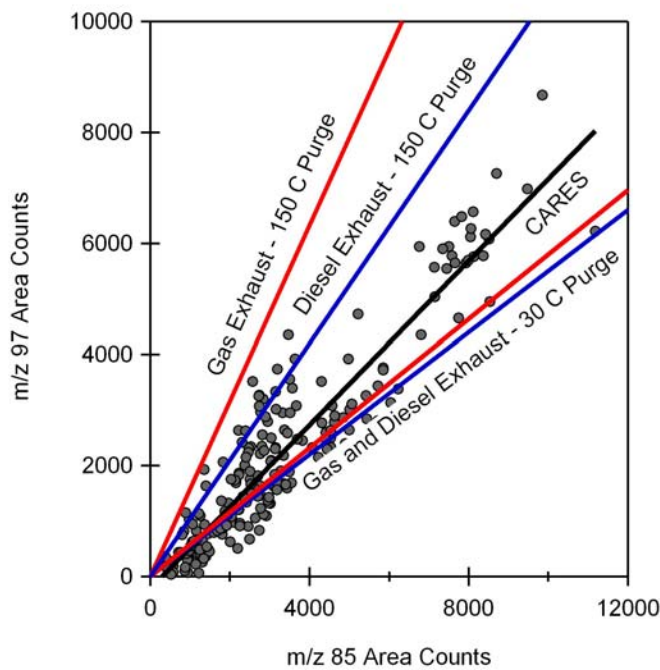


**Figure 12.** Correlation between m/z 97 and m/z 85 during CARES. The diesel and gasoline reference lines are the m/z 97 to m/z 85 ratios found from the exhaust spectra displayed in Figure 6. The CARES data yield a mass 97 to 85 ion intensity ratio of 0.74, which lies in between the 30 C and 150 C purge ratios.